https://doi.org/10.5194/nhess-2019-314
Preprint. Discussion started: 25 September 2019

Natural Hazards and Earth System Sciences
Discussions

Meteorological drought in the Miño-Limia-Sil hydrographic demarcation: The role of atmospheric drivers

Rogert Sorí[1], Marta Vázquez[1,2,3], Milica Stojanovic[2,3], Raquel Nieto[1], Margarida Liberato[2,3], Luis Gimeno[1],

[1]Environmental Physics Laboratory (EPhysLab), CIM-UVigo, Universidade de Vigo, Ourense, 32004 Spain

[2]Instituto Dom Luiz, Faculdade de Ciências da Universidade de Lisboa, Campo Grande, Portugal

[3]Escola de Ciências e Tecnologia, Universidade de Trás-os-Montes e Alto Douro, Vila Real, Portugal

Correspondence to: Rogert Sorí (rogert.sori@uvigo.es)

Abstract. Drought is one of the main natural hazards because of its environmental, economic, and social impacts. Therefore, its study, monitoring and prediction for small regions, countries, or whole continents are challenging. In this work, the meteorological droughts affecting the Miño-Limia-Sil Hydrographic Demarcation (MLSHD) in the northwestern Iberian Peninsula during the period of 1980–2017 were identified. For this purpose, and to assess the combined effects of temperature and precipitation on drought conditions, the Standardised Precipitation-Evapotranspiration Index (SPEI) was utilised. During the study period there was no trend in the series of SPEI at the temporal scale of 1 mo (SPEI1); however, the number of drought episodes and their severity have been increasing historically, but this metric was not statistically significant. Particular emphasis was given to investigating atmospheric circulation as a driver of different drought conditions. To this aim, a daily weather type classification was utilised for the entire Iberian Peninsula. The results showed that atmospheric circulation from the southwest, west, and northwest were directly related to dry and wet conditions in the MLSHD during the entire climatological year. Contrastingly, weather types imposing atmospheric circulation from the northeast, east, and southeast and pure anticyclonic circulation were negatively correlated with the SPEI1. In this sense, the major teleconnection atmospheric patterns related to dry/wet conditions were the Arctic Oscillation, Scandinavian Pattern, and North Atlantic Oscillation. Dry and wet conditions according to the SPEI at shorter temporal scales were closely related to the soil moisture in the root zone, and also strongly influenced the streamflow of the Miño and Limia rivers, especially during the rainy season. However, a direct relationship between soil moisture and streamflow was also observed when dry/wet conditions accumulated for more than 1 y. We concluded that regional patterns of land-use change and moisture recycling are important to consider in explaining runoff change, integrating land and water management, and informing water governance.

https://doi.org/10.5194/nhess-2019-314
Preprint. Discussion started: 25 September 2019

Natural Hazards and Earth System Sciences
Discussions

1. Introduction

Drought is considered a major natural hazard in many regions worldwide, as it affects a wide range of economic, social, and environmental sectors (Wilhite, 2000; McMichael et al., 2011; Stankeet et al., 2013; Gerber and Mirzabaev, 2017; Guerreiro et al., 2018). This phenomenon is usually considered a prolonged dry period in the natural climate cycle; it is initially caused by a lack of rainfall as well as thermodynamics factors, and can occur anywhere in the world (WMO & GWP, 2016; Vicente-Serrrano et al., 2010). The Iberian Peninsula (IP) in the Euro-Atlantic and Mediterranean regions is a drought-prone area that has presented a significant tendency towards dryness during 1901–1937 and 1975–2012 (Páscoa et al., 2017). The impacts of drought have been widely investigated in this region, and range from impacts on river streamflow (Lorenzo-Lacruz, 2013), productivity of rainfed crops (Peña-Gallardo et al., 2019), forests (Gouveia et al., 2009; Barbeta and Peñuelas, 2016; Vidal-Macua et al., 2017; Peña-Gallardo et al., 2018), and even human mortality in Galicia, northwestern Spain (Salvador et al., 2019).

Terrestrial ecosystems often vary significantly in their responses to drought (Knapp et al., 2015). The IP is characterised by different climate types, from a humid Atlantic climate in the northwest and north to semi-arid Mediterranean conditions in the east and southeast (e.g. Parracho et al., 2016), and strong seasonal variability (Serrano et al., 1999). Therefore, regional-scale studies have the advantage of better characterising the phenomenon of drought and its impacts, thereby supporting the reduction of the vulnerability and losses induced by drought. The northwestern Iberian Peninsula (NWIP) is a hydrologically important region of the IP where water resources of the Miño-Sil and Limia river basins represent an important source of benefits for local agricultural production (CHMLS, 2017). Vicente-Serrano et al. (2011) revealed that both the precipitation (P) and potential evapotranspiration (PET) increased in the period from 1930 to 2006 over the NWIP, but the mean duration of drought episodes increased by approximately 1 mo in the last 30 y of this period as a consequence of the increase in the PET (differences are not statistically significant). Thus, temperature, wind, and relative humidity are also important factors to include in characterising drought (Vicente-Serrano et al., 2010; WMO, 2012). Over a shorter study period (1974–2010), Gómez-Gesteira et al. (2011) found a significant increasing trend in land and sea surface temperatures of 0.5 °C and 0.24 °C per decade, respectively, but annual P did not show any trend in the NWIP. There is concern owing to the high confidence level that global warming is likely to reach 1.5 °C above preindustrial levels in a short period (between 2030 and 2052) if it continues to increase at the current rate (IPCC, 2018). The IP is considered one of the European regions that is most likely to suffer an increase in drought severity during the 21st century (Vicente-Serrano et al., 2011). However, Trenberth et al. (2014) argued that increased heating from global warming may not cause droughts, but it is expected that when droughts occur they are likely to occur more quickly and be more intense.

The climate of the Euro-Atlantic sector is characterised by considerable variability over a wide range of time scales (Visbeck et al., 2001; Sousa et al., 2016; Abrantes et al., 2017). Atmospheric drivers of P and their impact on the availability of water

https://doi.org/10.5194/nhess-2019-314
Preprint. Discussion started: 25 September 2019

Natural Hazards and Earth System Sciences
Discussions

resources in the IP have been investigated through weather type (WT) classifications (e.g. Ramos et al., 2014), identification of blocking events (Sousa et al., 2016), and assessments of climatic teleconnection patterns, such as the North Atlantic Oscillation (NAO) (Muñoz-Díaz and Rodrigo, 2004; Trigo et al., 2004; deCastro et al., 2006), which is considered a dominant mode of climate variability for Europe (Visbeck et al., 2001), the Arctic Oscillation (AO) (deCastro et al., 2006), El Niño Southern Oscillation (ENSO) (Vicente-Serrano, 2005), and Scandinavian Pattern (SCAND) (deCastro et al., 2006). For hydrological purposes, the Miño-Limia-Sil Hydrographic Demarcation (MLSHD) is considered of importance for the northern provinces of Portugal and Galicia in the NWIP and a homogeneous region in terms of the total P variance over the IP (Rodriguez-Puebla et al., 1998) and consequently the influence of droughts (Russo et al., 2015). The MLSHD extends from approximately 41°N to 44°N and from 6.5°W to 9°W, and covers an area of approximately 20 000 km^2 in the NWIP (Figure 1), including the territories of Spain (Galicia) and northern Portugal. It is considered a management unit where the terrestrial area is composed of the Miño-Sil and Limia river basins and the transitional, subterranean, and coastal waters associated with said basins (CHMLS, 2017). In the Spanish part of the MLSHD, the water demands of agrarian use represent 73.2% of the total water demand (Vargas and Paneque, 2019). In our search, we did not find any study considering the MLSHD as a whole. Therefore, our aim was to investigate the occurrence of meteorological drought and its propagation across the hydrological cycle in the MLSHD (Figure 1), as well as the atmospheric mechanisms of drought onset and termination. We expect that our results will contribute to increase the hydroclimate knowledge of the region and support early drought warning in order to develop effective mitigation strategies for the MLSHD.

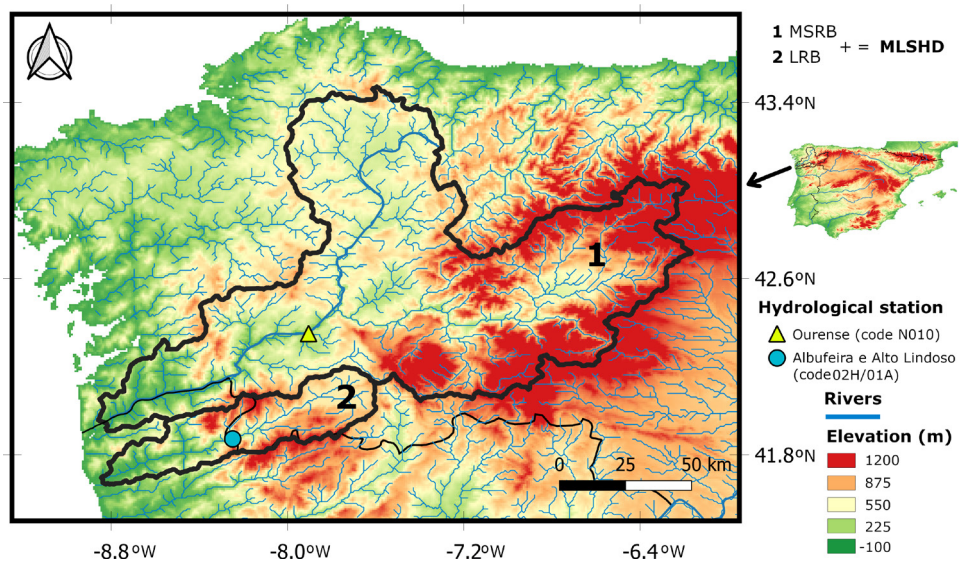

Figure 1. Geographic location and boundaries (black lines) of the Miño-Sil River Basin (MSRB) (1) and Limia River Basin (LRB) (2), which conform to the Miño-Limia-Sil Hydrographic Demarcation (MLSHD). The rivers are represented by blue lines, and shaded colours (green to red) represent the elevation (in meters above sea level) from the HydroSHEDS project (Lehner et al., 2011).

https://doi.org/10.5194/nhess-2019-314
Preprint. Discussion started: 25 September 2019

Natural Hazards and Earth System Sciences
Discussions

2. Materials and methods

2.1 Drought identification

There are many drought indices and different criteria for the best approach to detect and investigate droughts (Svodoba and Fuchs, 2016). Here, the Standardised Precipitation-Evapotranspiration Index (SPEI) (Vicente-Serrano et al., 2010) was utilised to determine the occurrence and evolution of dry and wet conditions in the MLSHD. The SPEI is based on the same methodology of the Standardised Precipitation Index (SPI) (Mckee et al., 1993), but it has the advantage over common P-based drought indices of considering the effects of temperature in the monthly climatic water balance (P minus reference evapotranspiration (Eto)). In the absence of meteorological data required for applying the Penman-Monteith equation, which is recommended by the Food and Agriculture Organization (FAO) of the United Nations in the FAO Bulletin 56 (Allen et al., 1998), we used the method proposed by Hargreaves and Samani (1985) based on temperature data to estimate the Eto according to Equation 1:

$$Eto = a \text{ x } Ra \text{ x } \left(\sqrt{Tx - Tn}\right) + (Tm + 17.8) \quad (1)$$

The resultant values of the water balance were standardised using a three-parameter log-logistic distribution to obtain the SPEI, which was adapted to frequencies from 1 mo to 24 mo. The SPEI is a multiscale index that allows the assessment of the response of different hydrological systems and ecosystems to drought (Vicente-Serrano et al., 2010). The SPEI has been widely utilised for identifying dry and wet conditions and evaluating drought impacts, recurrence, and variability, among others. It was also chosen for this study because the results of Vicente-Serrano et al. (2014) described how drought severity has increased in the past five decades (1954–2014) in natural, regulated, and highly regulated basins of the IP as a consequence of greater atmospheric evaporative demand resulting from temperature rise. A classification of drought categories according to SPI values and the classification proposed by Agnew (2000) (Table 1) was utilised in this study. Other authors have also employed this classification for investigating drought in the IP (e.g. Pascoa et al., 2017). Drought episodes affecting the MLSHD were identified. A drought episode was considered to occur when the SPEI at the temporal scale of 1 mo fell below zero, reached a value of at least -0.84, and later returned to positive values.

Table 1. Standardised Precipitation-Evapotranspiration Index (SPEI) classification according to Agnew (2000).

SPEI	Probability	Category
> 1.65	0.05	Extremely humid
> 1.28	0.10	Severely humid
> 0.84	0.20	Moderately humid
> -0.84 and < 0.84	0.60	Normal
< -0.84	0.20	Moderately dry

https://doi.org/10.5194/nhess-2019-314
Preprint. Discussion started: 25 September 2019

Natural Hazards and Earth System Sciences
Discussions

< -1.28	0.10	Severely dry
< -1.65	0.05	Extremely dry

2.2 The Standardised Streamflow Index

The Standardised Streamflow Index (SSI) (Vicente-Serrano et al., 2012) was used for assessing the possible impact of the propagation of dry and wet conditions accumulated from several temporal scales through the hydrological cycle over the streamflow of the Miño and Limia rivers. According to these authors, one advantage of the SSI is that it is measured in the same units that are used for other climatological drought indices, such as the SPI and SPEI, thereby allowing comparisons between hydrological and climatological droughts.

2.3 Weather type computation

The dominant climate in any region is largely a consequence of and can be linked to frequent synoptic systems throughout the year. The synoptic systems represent the general circulation of the atmosphere through different configurations of variables. For this reason, an objective classification scheme based on the methodology adopted by Trigo and DaCamara (2000) was utilised to obtain the dominant circulation weather types (CWTs), which modulate the IP climate. The method uses daily sea level pressure (SLP) values obtained by the ERA-Interim reanalysis for the period of 1989–2017 on different points over the IP in order to construct a set of indices associated with the direction and vorticity of the geostrophic flow, namely total shear vorticity (Z), southerly shear vorticity, easterly shear vorticity, total flow (F), southerly flow (SF), and westerly flow (WF). The area used to compute WTs was the same as that used by Ramos et al. (2014). Further details about the computation of the indices and the rules adopted to defined the WTs over the IP can be found in Ramos et al. (2014) and Trigo and DaCamara (2000). According to the methodology developed by Trigo and Da Camara (2000), 10 different "pure" CWTs can be identified, namely Northeastern (NE), Eastern (E), Southeastern (SE), Northwestern (NW), Western (W), Southwestern (SW), North (N), South (S), Anticyclonic (A), and Cyclonic (C). Pure directional WTs were those showing $|Z| < F$ with the direction defined by $\tan^{-1}$ (WF/SF) (180° added if WF is positive). If $|Z| > 2F$, then the circulation would be considered C (if $Z > 0$) or A (if $Z < 0$). Additionally, 16 hybrid circulations could be defined as a combination of A and C circulation with directional CWTs. In this case, $F < |Z| < 2F$.

2.4 Wavelet coherence analysis

Wavelet coherence (WC) analysis is used to identify which frequency bands within two time series are co-varying (Torrence and Webster, 1999). This definition is similar to that of a traditional cross correlation, and the WC can be considered as a localised correlation coefficient in time-frequency space (Torrence and Compo, 1998; Grinsted et al., 2004). For this assessment, the SPEI at the temporal scale of 1 mo (SPEI1) and six monthly series of teleconnection patterns, namely the bivariate ENSO time series (BEST) (Smith and Sardeshmukh, 2000) and Atlantic Multidecadal Oscillation (AMO) (Enfield

https://doi.org/10.5194/nhess-2019-314
Preprint. Discussion started: 25 September 2019

Natural Hazards and Earth System Sciences Discussions

et al., 2001) (available at https://www.esrl.noaa.gov), NAO, AO, East Atlantic (EA), and SCAND (https://www.cpc.ncep.noaa.gov/data/teledoc/telecontents.shtml), were utilised by initially applying Equation 2, as follows:

$$R_n^2(S) = \frac{\left|S\left(s^{-1}W_n^{XY}(s)\right)\right|^2}{S\left(s^{-1}\left|W_n^X(s)\right|^2\right) * S\left(s^{-1}\left|W_n^Y(s)\right|^2\right)} \quad (2)$$

where S is a smoothing operator and XY are the two series. The WC ranges from 0 to 1; if the value is closer to 1, then the correlation between the two series is higher. An advantage of WC over the classical cross-correlation analysis is that the phase relationship is calculated such that the degree to which two time series are positively or negatively related can be measured as both a function of time and period (Shulte et al., 2016).

2.5 Datasets

Monthly gridded data of P and maximum and minimum temperature (Tx and Tn, respectively) were obtained from daily values of the E-OBS gridded dataset (Cornes et al., 2018) with a resolution of 0.1° in longitude and latitude for the period of 1980–2017. This period was set for all the analyses in this study. These series were also utilised to compute the SPEI in the MLSHD. For the WT computation, daily values of SLP were utilised from the ERA-Interim reanalysis datasets (Dee et al., 2011) with a resolution of 1° for the region between 25°N–70°N and 45°E–45°W. The eastwards and northwards vertically integrated moisture flux was utilised to compute the Vertical Integral Moisture Flux (VIMF) anomalies and its divergence anomalies.

To investigate the drought propagation, monthly root-zone soil moisture (SMroot) data at a resolution of 0.25° × 0.25° from the Global Land Evaporation Amsterdam Model (GLEAM v3.2a) were utilised (Martens et al., 2017; Miralles et al., 2011). Monthly values from daily values of the Miño River discharge registered at the hydrological station N010 in Ourense and monthly values of river discharge from the Limia River at the hydrological station of Albufeira Do Alto Lindoso in northern Portugal (Figure 1) for the period of 1992/1993–2017 were also utilised to calculate the SSI. These data belong to the Confederación Hidrográfica del Miño-Sil in Spain (https://www.chminosil.es/es/ide-mino-sil) and the National System of Water Resources Information (https://snirh.apambiente.pt/) of Portugal, respectively. SPEI values from 1 mo to 24 mo temporal scales were correlated with the SSI to determine the impact of accumulated dry and wet conditions on the rivers' streamflow.

https://doi.org/10.5194/nhess-2019-314
Preprint. Discussion started: 25 September 2019

Natural Hazards and Earth System Sciences
Discussions

3. Results

3.1 Representative hydroclimatic regime in the Miño-Limia-Sil Hydrographic Demarcation

The annual cycle of P, Tmax, and Tmin along the hydrological year (October–September) in the MLSHD is shown in Figure 2. P showed a very high temporal variability across the annual cycle, and was greater than 100 mm from October to February. During winter, the large-scale circulation is mainly driven by the position and intensity of the Iceland Low, and western Iberia is affected by westerly winds that bring humid air and generate P (Trigo et al., 2004). The movement of the sub-tropical anticyclone to the south leaves the region open to the influence of the frontal systems from the west, which are responsible for most of the P. Synoptic-scale baroclinic perturbations from the Atlantic Ocean are responsible for most of the P between October and May (DeCastro et al., 2006). After February, the P is lower and reaches the minimum value (P < 30 mm) in July. Summer is predominantly influenced by high pressures of the eastern sub-tropical cyclone, which determine air subsidence and consequently atmospheric stability (PGRH, 2016). The annual cycle of Tx and Tn revealed a cycle opposite to that of P. Minimum monthly values of Tx (< 9 °C) and Tn (2 °C) occurred in December and February, while the maximum values occurred in July and August (> 24 °C).

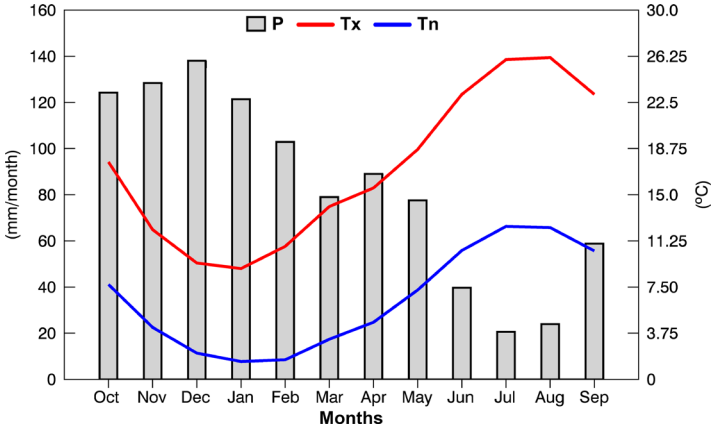

Figure 2. Annual cycle of precipitation (grey bars) and maximum (red line) and minimum (blue line) temperature in the Miño-Limia-Sil Hydrographic Demarcation from 1980–2017.

3.2 Drought conditions

Figure 3a shows the temporal evolution of the SPEI1 computed for the MLSHD during 1980–2017. The high variability of the series made it difficult to identify the most extensive and intense periods affected by dry or wet conditions. However, dry conditions prevailed in periods such as 1989–1992, 2004–2005, and 2015–2017, which was in agreement with results obtained by other authors for the NWIP through different indices, who also reported them for several time scales (e.g. Garcia-Herrera, 2007; Andrade and Pereira, 2015; Spinioni et al., 2016; Ojeda et al., 2019). At this scale, the negative values of the SPEI are primarily related to meteorological drought, which is unable to diagnose the agricultural, hydrological, and socioeconomic

https://doi.org/10.5194/nhess-2019-314
Preprint. Discussion started: 25 September 2019

Natural Hazards and Earth System Sciences
Discussions

types of drought. However, it is an indicator that can be perceived as the initial cause because these types of drought are triggered by the deficit of P combined with high temperatures and significant Eto. The identification of meteorological drought episodes affecting the IP has been a topic of research during the last few years (e.g. Lana et al., 2006; Lorenzo-La Cruz et al., 2013; González-Hidalgo et al., 2018). The threshold of -0.84 (dashed line in Figure 3) identifies the moments in which the criterion is met for a drought episode occurring in the MLSHD. The onset, termination, and length of these episodes are shown in Figure 3b. According to the visual analysis, the length of these episodes increased after 2003.

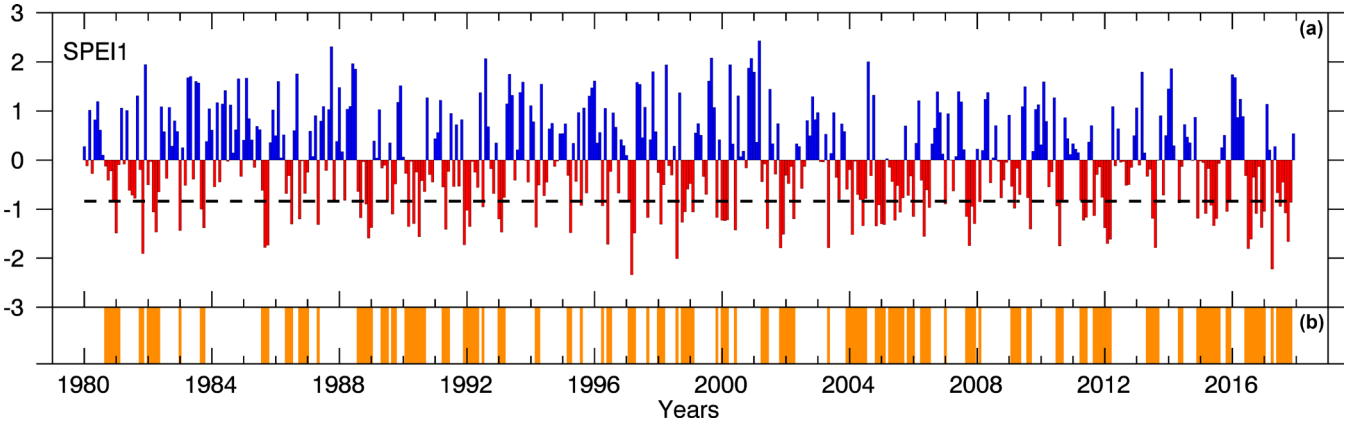

Figure 3. Wet (blue bars) and dry (red bars) conditions according to the Standardised Precipitation-Evapotranspiration Index at the 1 mo temporal scale (SPEI1) (a) and dry episodes (orange bars) (b) during 1980–2017.

A trend analysis revealed a small statistically significant ($p < 0.05$; calculated using the Wald test with t-distribution of the test statistic) trend in the series of the SPEI1 during the period of 1980–2017 (Table 2). Vicente-Serrano et al. (2011) found that the mean duration of drought episodes in the NWIP increased by approximately 1 mo in the last 30 y of 1930–2006 as a consequence of the increase in PET (differences are not statistically significant). However, for a longer period (1950–2010), the NWIP was affected by a decrease in the number of consecutive wet days (Casanueva et al., 2014). According to our results, the duration of the drought events over the MLSHD increased at a rate of 0.02 mo/y in the last 37 y. For the same period, the severity increased at a rate of 0.03 mo/y and the number of episodes was 0.01/y. However, none of these results were statistically significant. The trends were analysed by taking into account the mean value for each of the events starting in a specific year for the period of 1980–2017.

Table 2. Trend analysis of the 1 mo Standardised Precipitation-Evapotranspiration Index (SPEI1) series and the duration, severity, and number of events per year. The slope represents the trend, and significant trends are marked with an asterisk. Significance is calculated using the Wald test with t-distribution of the test statistic, and the trend is considered significant when $p < 0.05$.

	Slope	Units	*p* value
SPEI1	-0.0009*	y^{-1}	0.009

https://doi.org/10.5194/nhess-2019-314
Preprint. Discussion started: 25 September 2019

Natural Hazards and Earth System Sciences
Discussions

Number of Episodes	0.01	episodes/y	0.260
Duration	0.02	mo/y	0.520
Severity	0.03	y^{-1}	0.260

Drought events disrupt food production systems and can be a significant natural trigger for famine (Wilhite, 2000). The top 10 driest episodes in the period under study according to their severity are shown in Table 3. This selection was created to develop further analysis based on extreme meteorological dry conditions.

Table 3. The 10 most severe drought episodes that affected the Miño-Limia-Sil Hydrographic Demarcation from 1980 to 2017. The drought episodes are organised based on their severity from high to low, and the onset, termination, peak, and duration are shown.

Episode	Onset	Termination	Peak	Duration	Severity
E1	Jun/2016	Jan/2017	-1.80	8	7.7
E2	Sep/2011	Mar/2012	-1.70	7	7.0
E3	Dec/2014	Aug/2015	-1.34	9	6.1
E4	Dec/2003	Jul/2004	-1.52	8	6.0
E5	Feb/1990	Sep/1990	-1.56	8	5.8
E6	Aug/1988	Jan/1989	-1.60	6	5.7
E7	Jun/2017	Nov/2017	-1.66	6	5.6
E8	Nov/2001	Apr/2002	-1.80	6	5.4
E9	Sep/2007	Dec/2007	-1.74	4	5.1
E10	Dec/1991	May/1992	-1.72	6	4.9

3.3 Relationship between the circulation weather type classification and drought conditions

The 10 pure CWTs responsible for the major variance in atmospheric circulation over the IP are shown in Figure 4. These patterns (obtained using the same methodology) have been previously used to investigate the relationships between the atmospheric circulation and P variability (e.g. Cortesi et al., 2014; Ramos et al., 2014) or drought conditions in the IP (e.g. Russo et al., 2015). We aimed to determine the association of large-scale atmospheric circulation over the IP with drought conditions that affected the MLSHD during 1980–2017. The reddish (blueish) isolines in Figure 4 identify the maximum (minimum) values of SLP. The NE configuration was characterised by a high-pressure system localised over the Atlantic Ocean northwest of the MLSHD. In the E and SE configuration, the high-pressure system was shifted northwards and centred over the Cantabrian Sea, in the E circulation it was centred over the Celtic Sea, and in the SE circulation it was centred over France and the southern UK. The NW and W WTs consisted of a high-pressure system east of the IP in the Atlantic Ocean and a low-pressure system over the Bay of Biscay and Cantabrian Sea. The high-pressure systems were intensified in the case of the NW configuration and covered more northern areas, and the low-pressure system was more developed in the case of the W configuration. In the SW WT, the high-pressure systems were limited to the most southern areas in the North Atlantic and

https://doi.org/10.5194/nhess-2019-314
Preprint. Discussion started: 25 September 2019

Natural Hazards and Earth System Sciences
Discussions

a well-developed low-pressure system was localised over most parts of the North Atlantic. In the N configuration, a high-pressure system occurred west of the IP and lower pressures occurred over Iceland and western Europe. The opposite occurred in the S WT, with high pressures over western Europe and low pressures over the North Atlantic. The A configuration consisted of a dipole with lower pressures over southwestern Europe and the southern North Atlantic and lower pressures over higher latitudes. Finally, the C WT was formed by a quadrupole with two low-pressure systems centred over the western IP and southern Greenland and two high-pressure centres over Great Britain and the southwestern North Atlantic.

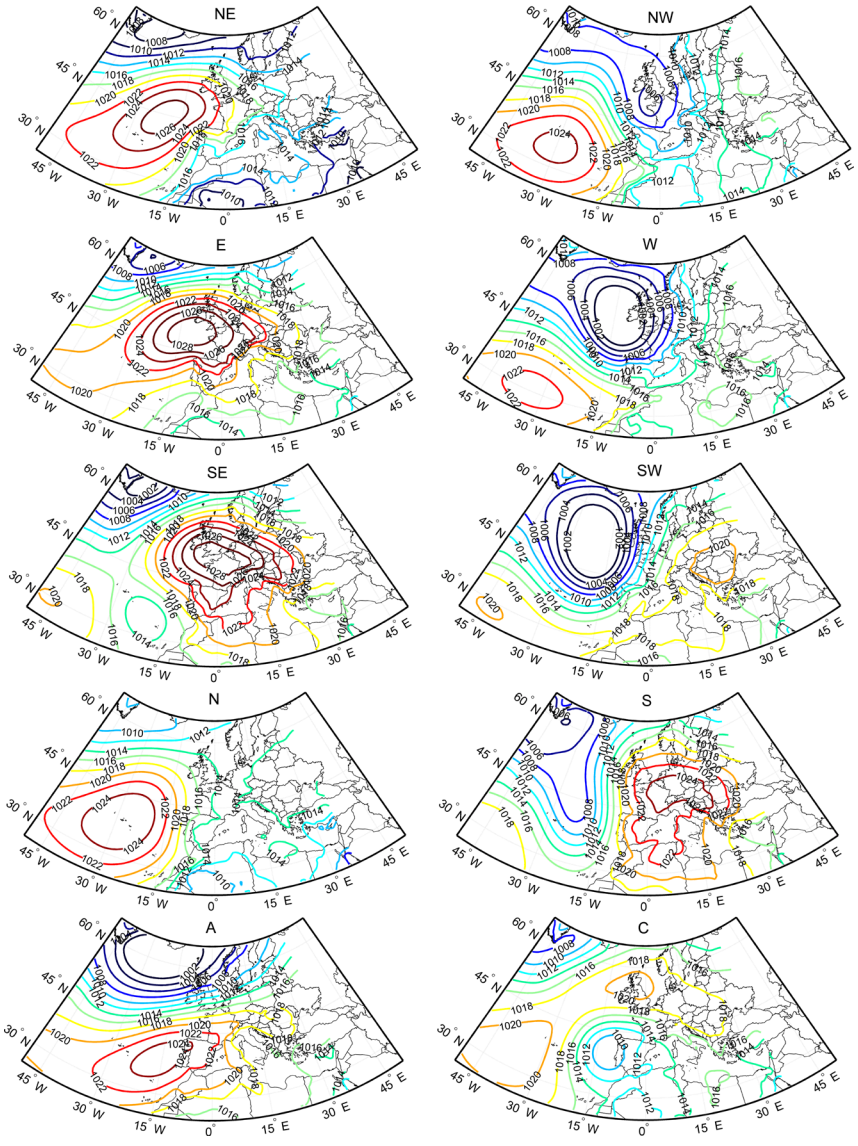

https://doi.org/10.5194/nhess-2019-314
Preprint. Discussion started: 25 September 2019

Natural Hazards and Earth System Sciences
Discussions

Figure 4. Mean sea level pressure field configuration of the 10 pure weather types (WTs) for the period of 1980–2017. The contour interval is 2 hPa.

The correlations between the monthly percentage of occurrence of each of the pure WTs and the SPEI1 time series are shown in Figure 5. The significant positive correlations found with the SW, W, and NW WTs are highlighted. The results suggested that air fluxes arriving from these directions were responsible for wetter conditions over the MLSHD, which was in agreement with the results of Russo et al. (2015), but for the NWIP. In addition, the C circulation appeared to be positively correlated with SPEI1; however, the correlations were not statistically significant. Contrastingly, the atmospheric circulation associated with the frequency of NE, E, and SE WTs was negatively correlated with the SPEI1 time series, thereby suggesting that their predominance was directly related to the dry conditions over the target region. This also occurred with the SPEI1 and A circulation correlations; however, these were lower and not significant during several months. As expected, positive and negative correlations prevailed for almost all the months with frequent C and A circulation (with the exception of May, July, and August for A circulation and March, April, and August for C circulation); however, significant correlations were only found for the SPE1 and A circulation pattern.

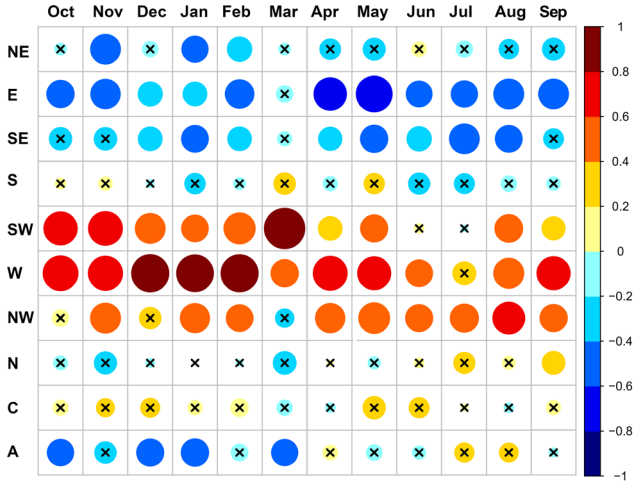

Figure 5. Correlations (statistically significant at $p < 0.05$) between the 1 mo Standardised Precipitation-Evapotranspiration Index and the monthly percentage of occurrence of each of the pure weather types for 1980–2017.

Similar results can be observed in Figure 6. This figure shows the anomaly in the percentage of occurrence for every WT presented during the 10 most severe events listed in Table 2. The anomaly was calculated for the complete duration of each drought event and referred to the 1980–2017 mean value for the same moths. For each of the events presented in the figure, the western CWTs showed negative anomalies. The largest anomalies appeared for the W circulation, and showed reductions of between 2.5% and 5.7% associated with the drought events. C circulation also decreased associated with drought events; however, the reduction was lower. Referring to the eastern CWTs, most of the episodes showed an increase in the percentage

https://doi.org/10.5194/nhess-2019-314
Preprint. Discussion started: 25 September 2019

Natural Hazards and Earth System Sciences
Discussions

of occurrence, especially for E circulation. The A, S, and N circulation showed positive and negative anomalies, which could have been associated with the time of year. Similar results were observed when the total number of severe events was considered (Figure S1).

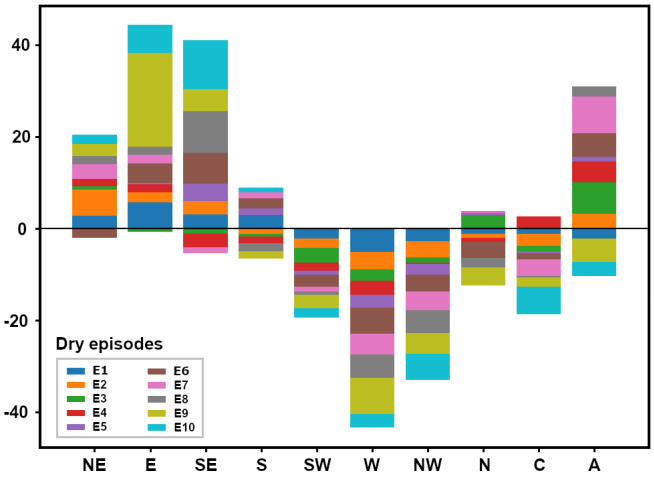

Figure 6. The anomaly in the percentage of each weather type associated with the 10 most severe drought episodes showed in Table 3.

In order to understand how distinct WTs might affect drought severity in the MLSHD, Figure 7 shows the monthly frequency (expressed in percentage) of each WT under different drought categories (moderately dry, severely dry, and extremely dry) according to the SPEI classification shown in Table 1. The months of October under moderately dry conditions were associated with the prevalence of A, E, and C circulation. Octobers affected by severely dry conditions were associated with a major percentage of A circulation, but for those under extreme drought conditions it seemed that E circulation highly increased with respect to previous drought categories, while there was a slight decrease in the frequency of A circulation. Additionally, the most frequent WT in the Novembers affected by moderate, severe, and extreme drought conditions was A circulation, which imposed an atmospheric flux from the north. For severely and extremely dry months of December, the frequency of WTs changed with respect to those of previous months, and an increase in the percentage of SE circulation was observed. This WT was characterised by a high-pressure centre located in the north of France and the south of England. The months of January under moderate and severe drought conditions were characterised by a major percentage of atmospheric conditions governed by the A pattern. When the severity increased in February, the percentage of occurrence of A circulation decreased, while E circulation prevailed under moderate drought conditions together with NE and A circulation when February was affected by extreme drought conditions. The opposite occurred in March when the A WT increased from moderate to extreme drought. April is normally considered the beginning of the dry season; under moderately dry conditions, the predominant WT was **A** circulation, but under severely and extremely dry conditions, the most frequent WTs were E and SE circulation. In the

https://doi.org/10.5194/nhess-2019-314
Preprint. Discussion started: 25 September 2019

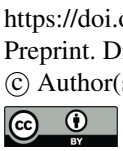

Natural Hazards and Earth System Sciences
Discussions

following months (May to September) affected by different drought categories, the combination of WTs E and A was the most frequent according to the percentage observed in the figure.

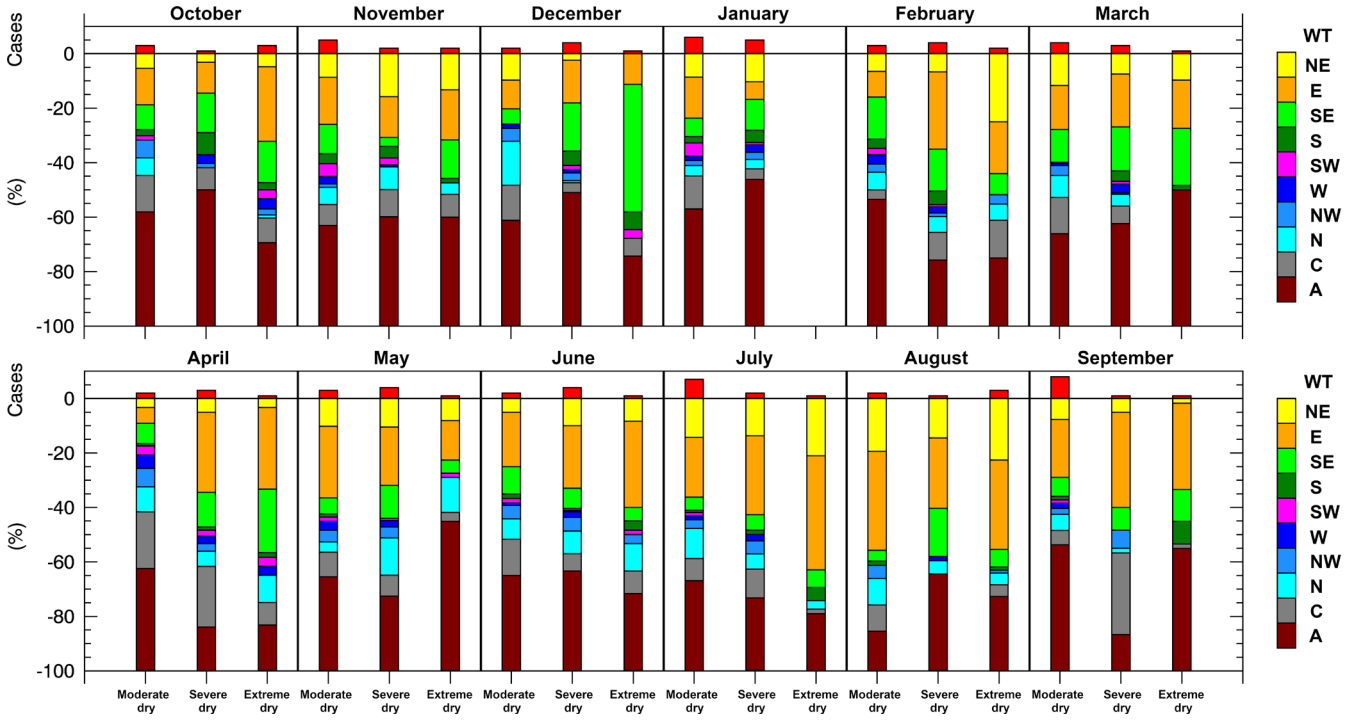

Figure 7. The anomaly of the percentage of occurrence of the 10 most severe events associated with each weather type (WT).

According to Drumond et al. (2011), the nature of rainfall variability over the north of Portugal and Galicia is associated with the moisture transport from two dominant moisture sources, namely the Bay of Biscay and the Tropical and Subtropical North Atlantic corridor; the latter extends from the Gulf of Mexico to Africa from 16°N to 40°N. Figures 8 and 9 show the anomaly of the VIMF and its divergence for the onset, peak, and termination of the drought episodes listed in Table 3. Episode 1 (E1) was the driest, and was characterised by anticyclonic circulation of the VIMF located to the southwest of the MLSHD, which moved to the north and imposed the moisture flux anomalies from the northeast. This was supported by prevailing A and NE WTs, which decreased in percentage when the drought condition disappeared in accordance with the increased frequency of C, W, and SW circulation and negative anomalies of the VIMF divergence. E2 began in September 2012 when intense positive anomalies of the VIMF divergence over the MLSHD suggested that divergence of the moisture flux prevailed, while A and NE WTs were the most frequent. The peak of this episode occurred in February 2012 when intense anticyclonic anomalies of the VIMF dominated the North Atlantic and had a centre to the north-northwest of the target region. In accordance, NE and E circulation were the most frequent over the IP. Drought conditions disappeared (in April 2012) when negative anomalies of the VIMF divergence affected the MLSHD, which was in association with cyclonic circulation anomalies of the VIMF with

https://doi.org/10.5194/nhess-2019-314
Preprint. Discussion started: 25 September 2019


Natural Hazards and Earth System Sciences
Discussions

the centre located over England. Correspondingly, the most frequent circulation patterns were C and NW. The third and fourth driest episodes began in December of 2014 and 2003, respectively. In both months, the most prominent circulation patterns were associated with A and C WTs. However, anticyclonic anomalies of the VIMF were observed over the North Atlantic and affected the MLSHD; these anomalies were more intense in December 2014 when positive anomalies of the VIMF divergence covered almost all the IP. The peak of E3 occurred with intense VIMF anomalies from the Atlantic Ocean that reached the northern portion of the IP; however, over the MLSHD, both negative and positive VIMF divergence anomalies were observed. The last month of E3 was August 2015; the SPEI changed to a positive value in September 2015 owing to negative anomalies of the VIMF divergence observed over the NWIP and the influence of C anomalies of the VIMF, which were in accordance with an increase in W circulation with respect to that in the previous stage of the episode. In the peak of E4, the VIMF anomalies indicated an increase associated with anticyclonic circulation in agreement of the major frequency of the A WT. This episode ended when the moisture flux from the west favoured the occurrence of convergence, despite the fact that the most frequent WT was A, followed by W. E5 began in February 1990 when the VIMF anomalies over the IP showed clear anticyclonic circulation accompanied by positive divergence anomalies and a high frequency of A circulation.

https://doi.org/10.5194/nhess-2019-314
Preprint. Discussion started: 25 September 2019

Natural Hazards and Earth System Sciences
Discussions

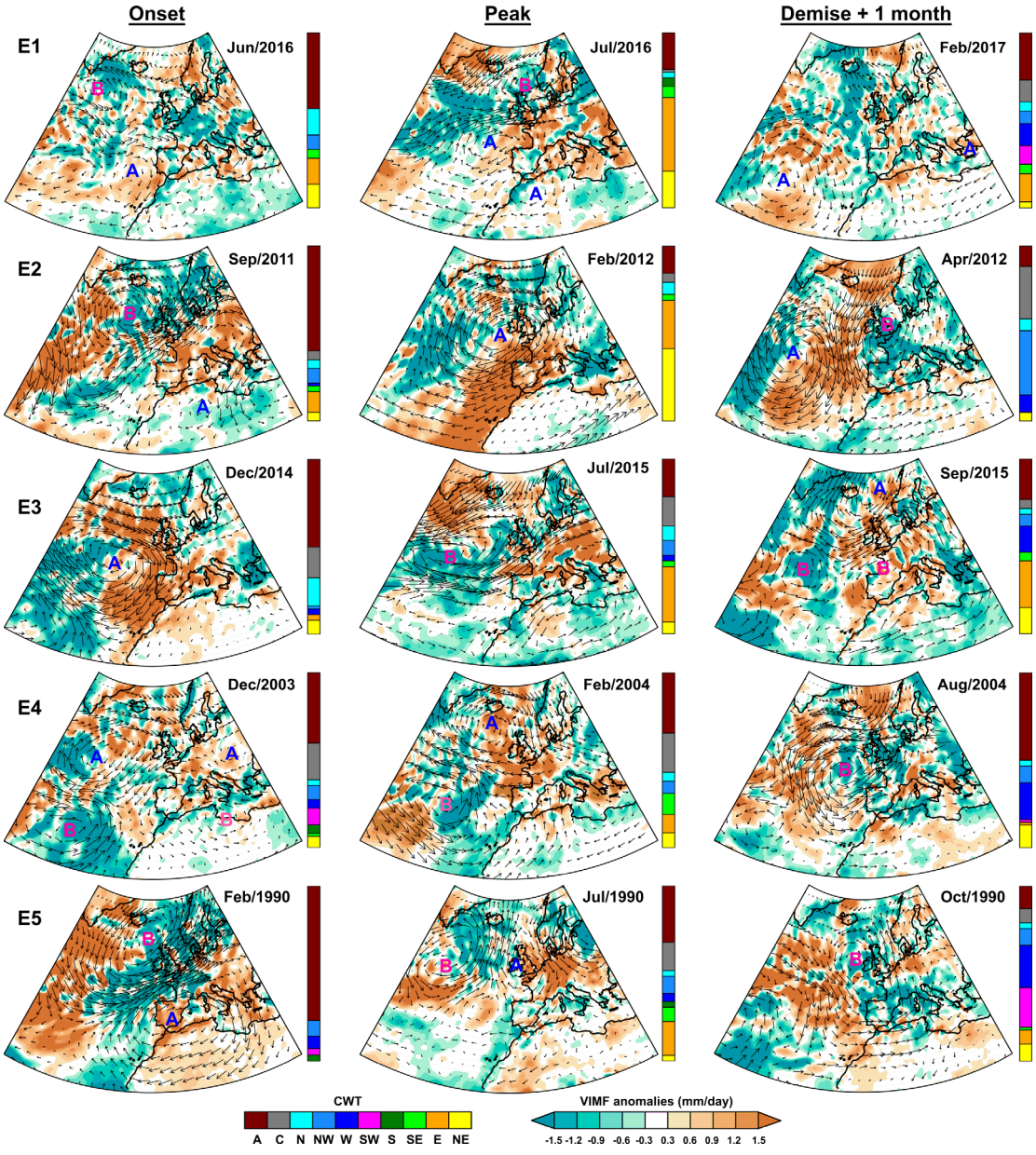

Figure 8. The monthly anomaly of the VIMF (in arrows) and its divergence (shaded) during 1980–2017 for the onset, peak, and 1 mo after the termination of each of the five most severe drought episodes (Es) shown in Table 3. Anticyclonic (cyclonic) centres of the VIMF anomaly circulations are represented as A (B). Vertical bars show the monthly percentage of each pure weather type (WT).

In Figure 9, the anomalies of the onset of E6 are shown; August 1988 was characterised by an anticyclonic circulation centre of the VIMF to the southwest of the MLSHD and cyclonic circulation in the northwest, which were both over the Atlantic Ocean (Figure 9). The VIMF divergence anomalies showed prevailing divergence conditions. The location of both centres was

https://doi.org/10.5194/nhess-2019-314
Preprint. Discussion started: 25 September 2019


Natural Hazards and Earth System Sciences
Discussions

opposite in the peak of the episode (December 1988), and the anticyclonic circulation of the VIMF was associated with an intense anticyclone in the NWIP that was in accordance with the major frequency of the A WT. This episode ended when the moisture flux was anomalous from the NW and negative anomalies of the VIMF divergence suggested the occurrence of convergence. In the onset of E7, as well as in E6, anomalous C circulation of the VIMF was observed with a centre located to the NW of Ireland. This situation changed at the peak of the episode with the prevailing frequency of A and NE WTs and anticyclonic circulation of the VIMF with the centre located to the northwest and near the MLSHD. When this centre moved westwards and the moisture flux anomalies arrived at the MLSHD from the north, which was shown in the WT, then dry conditions disappeared. In E8, the onset coincided with the peak of the episode. The atmospheric conditions in November 2001 revealed the prevalence of E and NE WTs and positive anomalies of the VIMF divergence associated with the anticyclonic circulation revealed by the VIMF anomalies over the North Atlantic Ocean to the northwest of the MLSHD. This episode ended in April 2002 owing to a positive SPEI1 value in May 2002, which was when the VIMF anomalies suggested that MLSHD received moisture flux from the combination of the cyclonic anomaly of the VIMF with the centre in Ireland and the anticyclone anomalies with a centre in the Atlantic Ocean and around 40°N. Owing to this combination, the WTs with the greatest prevalence were those that imposed circulation from the west. As well as in the previous episodes, in E9 and E10, the onset was characterised by anticyclonic anomalies of the VIMF with the centre located to the northwest of the MLSHD over the Atlantic Ocean, and both also showed a cyclonic circulation of the VIMF near the coast of northwest Africa and positive anomalies of the VIMF divergence over the MLSHD. In the onset of E9, the most frequent WTs were NE, E, and SE, while those in E10 were SE, A, and E. In E10, the peak was also in the onset and the VIMF anomaly patterns were very similar to those of the E9 peak with anticyclonic circulation to the northwest of the MLSHD near Ireland, which also occurred in the peaks of E2, E5, E6, and E7. Both episodes ended owing to negative anomalies of the VIMF divergence associated with VIMF anomalies from the west in E9 and C circulation in E10.

https://doi.org/10.5194/nhess-2019-314
Preprint. Discussion started: 25 September 2019

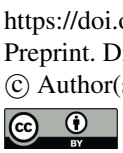

Natural Hazards and Earth System Sciences
Discussions

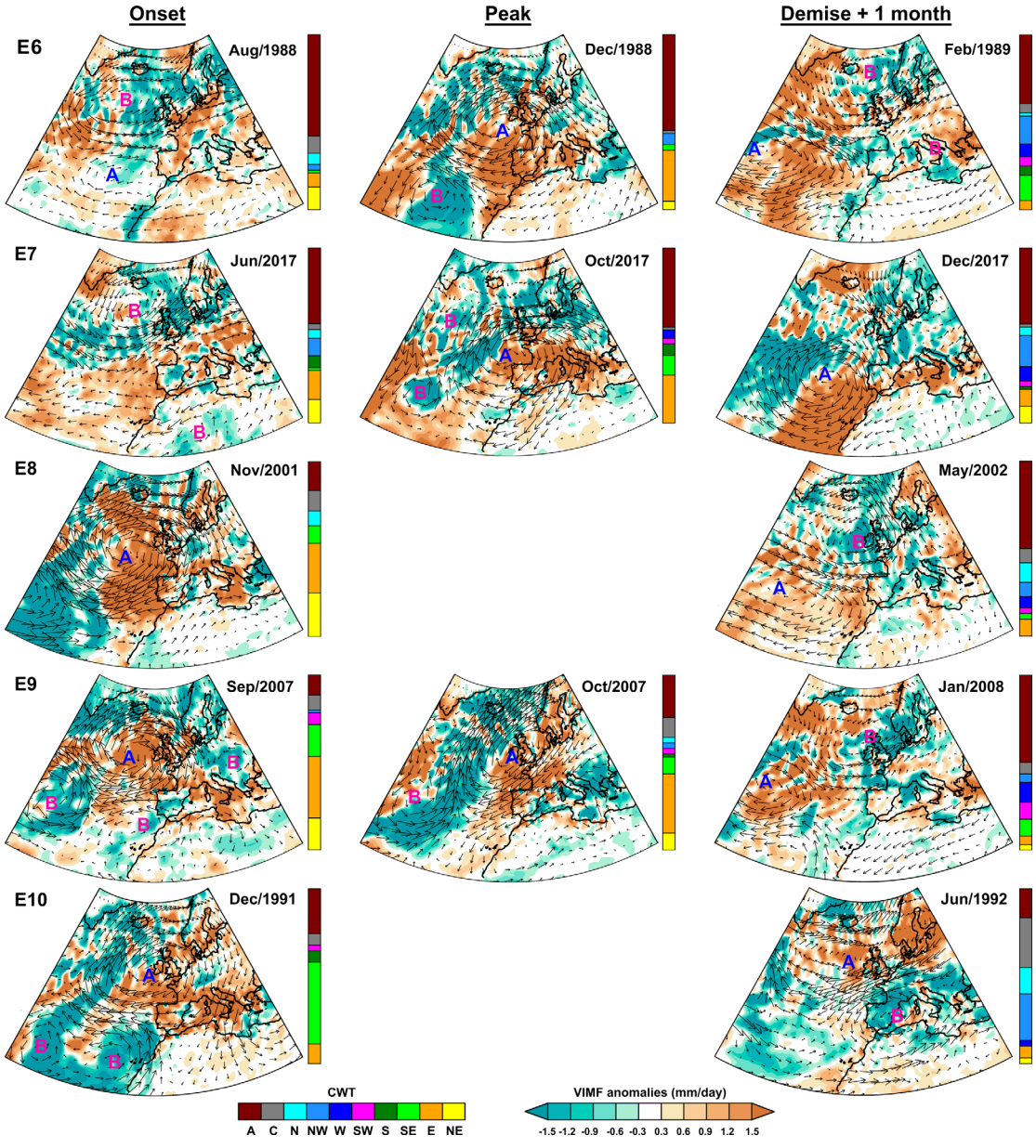

Figure 9. As Figure 8 but for Episode 6 to 10. For E8 and E10, the month of the onset is also the month of the peak.

3.4 Relationship between drought and modes of climate variability

Figure 10a shows the correlation between the BEST, NAO, EA, AO, SCAND, and AMO climatic indices with SPEI1 to 24 in order to determine any causal effect between atmospheric and oceanic teleconnection patterns and dry and wet conditions in

https://doi.org/10.5194/nhess-2019-314
Preprint. Discussion started: 25 September 2019


Natural Hazards and Earth System Sciences Discussions

the MLSHD. The results revealed a major link between the SCAND (positive correlation) and AO (negative correlation), particularly at short temporal scales (SPEI1 to SPEI4). This occurred because the SCAND pattern (initially referred to as the Eurasia-1 by Barnston and Livezey (1987)) in its positive phase was characterised by positive height anomalies, which sometimes reflected major blocking anticyclones, over Scandinavia and western Russia, but with weaker centres of the opposite sign over western Europe and eastern Russia, while the negative phase showed the opposite. On the contrary, the AO index is defined as the leading empirical orthogonal function using monthly mean 1000 hPa anomaly data over 20°N–90°N, and ranges from positive to negative values depending on the pressure anomalies in the Arctic region (Thompson and Wallace, 1998). In the case of the AO, its positive phase is characterised by a band of strong winds circulating around the North Pole, which keep colder air within the polar region and correspond to a deepening of the Azores High and the strengthening of the polar and subtropical jets over the Euro-Atlantic region (Ambaum et al., 2001). In the negative phase, this ring becomes weaker, thereby permitting the southwards penetration of Arctic air masses and an increase in the magnitude of the total eddy energy fluxes into the Euro-Atlantic region (Rivière and Drouard, 2015), which clearly affects the climatic conditions in the northwest IP (deCastro et al., 2006) and explains the negative correlations obtained with the SPEI. According to Wanner et al. (2001), the AO is similar to the NAO in many aspects. However, the NAO teleconnection is characterised by a meridional displacement of atmospheric mass over the North Atlantic area (usually expressed by the standardised air pressure difference between the Azores High and the Iceland Low) (Wanner et al., 2001). The negative phase of the NAO is associated with centre weakness of the Azores High and a southwards position in the storm tracks, thereby resulting in wet conditions over the IP (Trigo et al., 2002). Therefore, we also found negative correlations between the NAO and the SPEI for the 24 temporal scales.

In the case of the ENSO, namely the strongest ocean-atmosphere coupling phenomenon on the interannual time scale, at first the correlations between the SPEI were positive with the BEST index, but were very low (< 0.2) and not significant; these became negative when correlations were made with SPEI values computed from the past 6 mo to 24 mo, but were also not statistically significant. This suggested a poor association between the ENSO (El Niño and La Niña) and the occurrence of dry and wet conditions in the MLSHD. Nevertheless, according to Dai and Tan (2017), a warm (cold) ENSO enhances the negative (positive) AO phase, which is directly related to the MLSHD hydroclimate. Positive and insignificant correlations were found with the EA, and in the case of the AMO, the correlations were negative and decreased at major SPEI temporal scales.

Because the correlations in Figure 10a were greater with SPEI1 than with SPEI at other scales, a second correlation analysis was conducted in order to determine the relationships between the SPEI1 and the teleconnections, but at monthly scales (Figure 10b). The correlations with the BEST index were positive but low and not significant, except for in spring (March, April, and May) when the *r* values were negative. The results of Muñoz-Díaz and Rodrigo (2004) also showed that in winter, there is no ENSO influence, which is possibly because of the predominance of the NAO during spring, and La Niña leads to a low probability of drought in the north of the IP. Similar monthly correlations were obtained between the NAO and AO with SPEI1; however, as expected from the results of Figure 10a, it seemed that the AO was the most related to monthly dry and

https://doi.org/10.5194/nhess-2019-314
Preprint. Discussion started: 25 September 2019

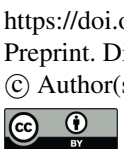

Natural Hazards and Earth System Sciences
Discussions

wet conditions in the MLSHD throughout the hydrological year, especially in the winter and spring months (December to May). This was in agreement with Mazano et al. (2019), who argued that the AO and NAO patterns have a significant impact on droughts in winter over large areas of the IP. However, these authors utilised the SPEI3. Positive correlations between the EA and SPEI1 were clearly observed from November to May. The results of Casanueva et al. (2014) also revealed a positive correlation between the EA index and P and the consecutive wet days over the NWIP during the boreal winter. The SCAND pattern was also positively correlated during all months of the year, but no significant correlations were found in December, February, and March. In a 300 mb height field typical for the positive phase of the SCAND, a weak trough appeared over the northeastern Atlantic in association with the centre of a major cyclonic anomaly and the North Atlantic storm-track activity as represented by the 850 mb polewards eddy heat flux, which weakened around Iceland and northern Europe, whereas the storm track extended eastwards into southern Europe through England (Bueh and Nakamura, 2007). Finally, there was no clear evolution of monthly correlations between the SPEI1 and AMO, and only significant negative correlations were found in August. Since the AMO was uncertain, it remained unknown whether it represented a persistent long-term periodic (10–30 y; 50–80 y) driver in the climate system (Knudsen et al., 2011), thereby affecting the IP weather at a longer periodicity (Abrantes et al., 2017).

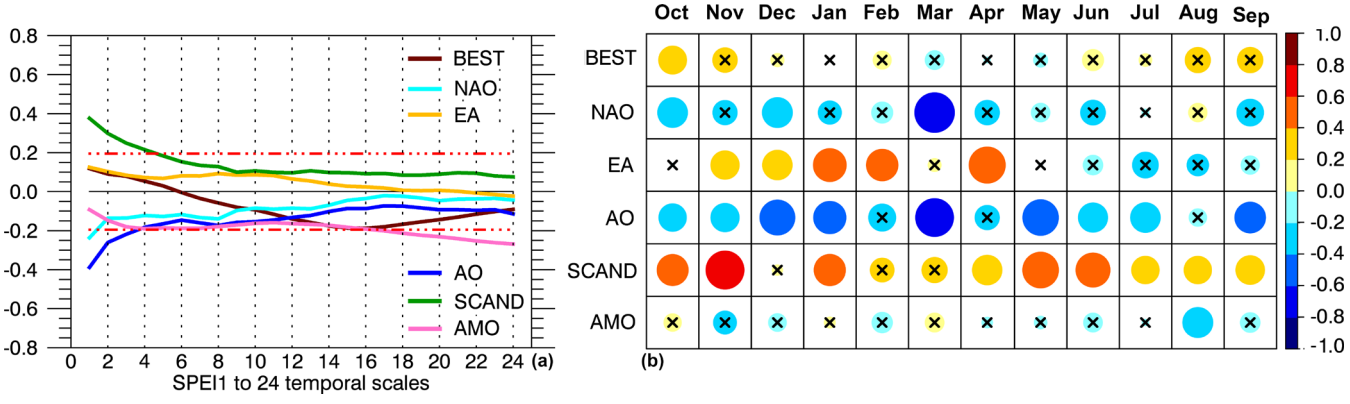

Figure 10. Correlation between the bivariate El Niño Southern Oscillation time series (BEST), North Atlantic Oscillation (NAO), East Atlantic (EA), Arctic Oscillation (AO), Scandinavian Pattern (SCAND), and Atlantic Multidecadal Oscillation (AMO) and the 1 mo Standardised Precipitation-Evapotranspiration Index (SPEI) at 24 temporal scales (a) and the monthly correlation between the same climate indices and the SPEI1 (b) for the period of 1980–2017.

The temporal variability of dry and wet conditions according to the SPEI1 in the MLSHD was also investigated by studying the potential links that may exist with climatic modes of variability for the BEST, EA, AMO, NAO, AO, and SCAND, but utilising a WC method. The results are shown in Figure 11. The coherence power between two series is shown as red to blue (strong to weak), and the black contours represent the locally significant ($p < 0.05$) power of the red-noise spectrum. The grey line depicts the cone of influence (COI), while the black arrows indicate the phase relationships between the climate indices

https://doi.org/10.5194/nhess-2019-314
Preprint. Discussion started: 25 September 2019

Natural Hazards and Earth System Sciences
Discussions

and SPEI1 and are denoted by arrows; those for in-phase point right, anti-phase point left, climate indices leading the SPEI1 by 90° point up, and SPEI1 leading the climate indices by 90° point down. The BEST showed strong but intermittently significant coherence with SPEI1 from year to year in the period of the 3–5 mo band, while a significant correlation was observed from 1980 to 1990 and for the 40–60 mo band, but it was outside the COI until the end of 1982. The vertical downwards arrows indicate that the SPEI1 series leads the BEST in phase by 90°. In the case of the EA and AMO, there was a frequent, significant co-oscillation with the SPEI1 in the high-frequency 0–6 y band. However, from approximately the end of the 2000s to 2012, there was a high coherence peak in the low-energy regions (for nearly 30–45 mo) between the EA and SPEI1. Negative coherent correlation occurred with the AMO after 63 mo from approximately 1996 to 2009.

The findings of Hurrell (1995) showed that the NAO has a rich combination of low frequencies from intraseasonal to interannual time scales and low frequency from decadal to multidecadal time scales. This signal was represented in positive coherence with the SPEI at high frequencies, as observed in Figure 11. This became strong between 4 mo and 12 mo in the periods of 1982–1984 and 2004–2012. At a longer temporal scale (30 mo to 34 mo), strong coherence was also observed in the period of 1986–1994. The authors argued the prominent role of the NAO in the NWIP climate. However, compared with those in the NAO, oscillations in the AO were manifested in the SPEI1 over most of the period on intermittent wavelengths from 2 mo to 6 mo, but most significantly from 6 mo to 36 mo (3 y) when the left-pointing arrows showed an anti-phase relationship (negative correlation), thereby indicating that the AO and SPEI1 moved in the opposite direction. Finally, the significant coherence between the SPEI1 and SCAND pattern revealed the recurring influence of this teleconnections pattern, particularly between 1991 and 2009 along with the 0–8 mo periodic bands and at low frequencies (from approximately 12 mo to 34 mo) during longer and continuous periods when right-pointing arrows showed a phase relationship.

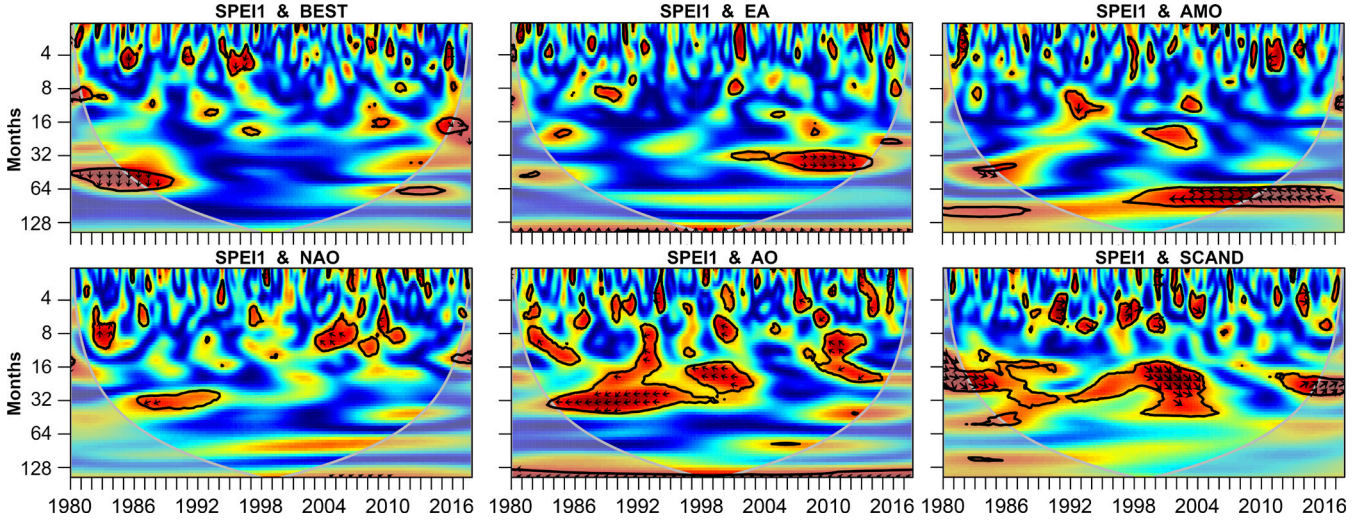

https://doi.org/10.5194/nhess-2019-314
Preprint. Discussion started: 25 September 2019

Natural Hazards and Earth System Sciences
Discussions

Figure 11. Wavelet coherence between the 1 mo Standardised Precipitation-Evapotranspiration Index (SPEI1) and the series of teleconnection patterns, namely the bivariate El Niño Southern Oscillation time series (BEST), East Atlantic (EA), Atlantic Multidecadal Oscillation (AMO), North Atlantic Oscillation (NAO), Arctic Oscillation (AO), and Scandinavian Pattern (SCAND). The colours from blue to red indicate the increasing coherence. Areas enclosed by a black line correspond to statistically significant cross-wavelet powers at the 95% level. The grey line depicts the cone of influence (COI). The black arrows indicate the phase condition. The phase relationships between the climate indices and SPEI1 are denoted by arrows for in-phase pointing right, anti-phase pointing left, climate indices leading the SPEI1 by 90° pointing up, and SPEI1 leading the climate indices by 90° pointing down.

3.5 Drought propagation

A deficit in P coupled with higher evaporation rates leads to a meteorological drought that may propagate into the soil up to the crops, thereby leading to an agricultural drought and a hydrological drought when both the groundwater and streamflow are affected. However, drought propagation through every component of the hydrological cycle depends on the severity of the drought event as well as the characteristics of the catchments (Van Lanen, 2006; Wang et al., 2016). We investigated the possible response of the SMroot (Figure 12a) and the streamflow (Figure 12b and c) due to drought conditions at several scales according to the SPEI1 to SPEI24. Figure 12a shows the maximum correlation values with the SPEI at the temporal scale from the previous 2 mo to 6 mo during the rainy season, and particularly in October, November, and December, thereby suggesting that the SMroot during the rainiest months also depended on dry/wet conditions from the dry season. From April to July, the highest correlations were more restricted to the previous 2 mo, while at the end of the dry season (August–September), this relationship increased with the SPEI, which was computed considering the accumulated balance from the previous 4 mo to 6 mo. Figure 12b and c focuses on the probable impact of drought conditions across several temporal scales over the main streamflow of the main rivers through the SSI values computed with the Miño River discharge recorded at the hydrological station in Ourense and the Limia River discharge registered at the hydrological station of Albufeira Do Alto Lindoso in northern Portugal, respectively. Positive and statistically significant correlations were mainly observed during the rainy season and with the SPEI from approximately 1 mo to 12 m in both locations, which indicated that in both locations, the streamflow during the rainy season could not be explained only by local P and may have been influenced by the long-term drought or wet conditions accumulated from previous months. The correlation patterns were very similar; however, in the driest months of July and August, the streamflow of the Miño River at Ourense seemed to be more dependent on dry/wet conditions beginning after the previous 6 mo until 24 mo. In contrast, for the same months, the correlations decreased for all temporal scales in Albufeira Do Alto Lindoso. The maximum correlations in these figures indicated the ideal climatic time scale over which to monitor hydrological droughts (Lorenzo-Lacruz et al., 2013). However, this relationship is complex and can vary as a function of several factors, including river basin features and water regulation (López-Moreno et al., 2013; Vicente-Serrano et al., 2014).

https://doi.org/10.5194/nhess-2019-314
Preprint. Discussion started: 25 September 2019

Natural Hazards and Earth System Sciences
Discussions

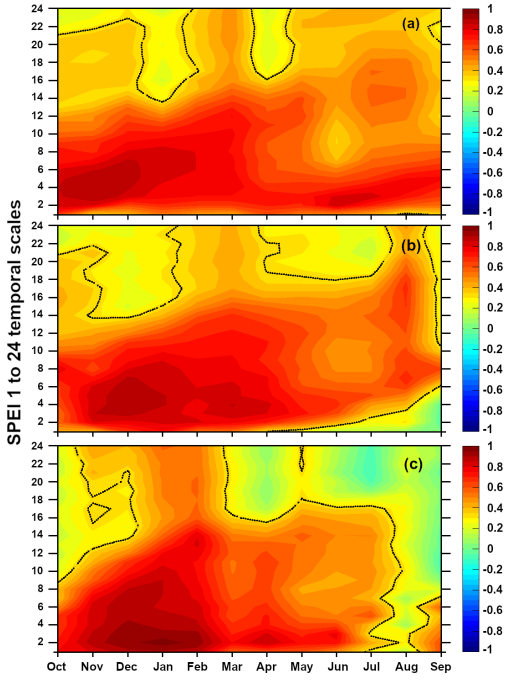

Figure 12. Monthly correlations among root-zone soil moisture (SMroot) anomalies for the entire Miño-Limia-Sil Hydrographic Demarcation (MLSHD) (a) and the Standardised Streamflow Index (SSI) for the Miño River (b) at the hydrological station of Ourense and that for the Limia River at the hydrological station of Albufeira do Alto Lindoso (c) with the Standardised Precipitation-Evapotranspiration Index (SPEI1 to SPEI24) in the MLSHD. Dotted lines represent significant correlations at $p < 0.05$. For (a) and (b) the analysis was performed for the period of 1980–2017 and for (c) the available period was 1992/1993–2017.

4. Conclusions

In this study, the temporal evolution of meteorological drought in the MLSHD and its relationship with different types of CWTs were investigated. For this reason, the SPEI was utilised at the temporal scale of 1 mo, which revealed that most frequent drought conditions affected the MLSHD in the periods of 1989–1992, 2004–2005, and 2015–2017. A daily WT classification for the entire IP was used to investigate the atmospheric circulation associated with different drought categories in the MLSHD. The results revealed the frequency of the WTs prone to dry conditions (A, SE, and E) and a general negative trend of C and west WTs (SW, W, and NW).

The most influential teleconnection patterns for dry but also wet conditions in the MLSHD were the AO and SCAND, followed by the NAO, which was in agreement with previous results for the region. Particularly, the AO and SCAND were also representative of a cause-effect relationship over stretches of the SPEI over longer periods and years. Considering that several studies have identified the NAO pattern as the dominant pattern for the Euro-Atlantic region and despite similarities between the AO and NAO representations discussed in the literature, the perspective that modulation of P and consequently dry

https://doi.org/10.5194/nhess-2019-314
Preprint. Discussion started: 25 September 2019

conditions in the MLSHD in the NWIP may be associated with the middle latitude jet stream and centres of action located over the Arctic and North Atlantic Ocean to the north of Spain. A periodic significant coherence between the SPEI1 and other teleconnection patterns (BEST, EA, and AMO) was also detected in the high-frequency region, and a linear correlation analysis for all SPEI temporal scales revealed that greater significant relationships occurred with the SPEI1, although in the case of the BEST and AMO they were not statistically significant. In conclusion, this study provided some information that is fundamental to understand the climate forcing of rainfall variability and the occurrence of dry conditions in the MLSHD, which is an important hydrological and socioeconomic region of the NWIP. Furthermore, these results will support hydrometeorological forecasting in the region.

Finally, drought conditions may affect the soil moisture and agricultural development in the area. This influence was higher in winter and lower in summer months, as the moisture availability was related to the drought cumulative effect on the previous 2 mo to 6 mo. From these results, it could be concluded that summer conditions may affect the moisture availability in humid months. Similar results were found for the river streamflow, as the SPEI1 to SPEI12 series were highly correlated with the river discharge in the humid months.

Acknowledgments

R.S acknowledge the support from the European Union and FEDER thought the RISC-ML project under the INTERREG España-Portugal program. R.S and M.S acknowledge the grant received from the European Association for Territorial Cooperation, Galicia Northern Portugal (AECP, GNP) thought the IACOBUS program in 2019. M.V is supported by the Xunta de Galicia under grant ED481B 2018/062. M.L and M.S are supported by the project "Weather Extremes in the Euro Atlantic Region: Assessment and Impacts-WEx-Atlantic" (PTDC/CTA-MET/29233/2017). This work is part of the LAGRIMA project (RTI2018-095772-B-I00) funded by Ministerio de Ciencia, Innovación y Universidades, Spain. Partial support was also obtained from the Xunta de Galicia under the Project ED431C 2017/64-GRC "Programa de Consolidación e Estructuración de Unidades de Investigación Competitivas (Grupos de Referencia Competitiva)".

References

1. Abrantes, F., Rodrigues, T., Rufino, M., Salgueiro, E., Oliveira, D., Gomes, S., Oliveira, P., Costa, A., Mil-Homens, M., Drago, T., and Naughton, F.: The climate of the Common Era off the Iberian Peninsula, Clim. Past, 13, 1901–1918, https://doi.org/10.5194/cp-13-1901-2017, 2017.
2. Agnew, C.T.: Using the SPI to identify drought, Drought Netw. News 2000, 12, 6–12, http://digitalcommons.unl.edu/droughtnetnews/1, 2000.
3. Allen, R. G., Pereira, L. S., Raes, D., and Smith, M.: Crop evapotranspiration: Guidelines for computing crop water requirements. FAO Irrigation and Drainage Paper 56, 300 pp., www.fao.org/docrep/X0490E/X0490E00.htm, 1998.

https://doi.org/10.5194/nhess-2019-314
Preprint. Discussion started: 25 September 2019

Natural Hazards and Earth System Sciences Discussions

4. Ambaum, M.H.P., Hoskins, B.J., and Stephenson, D.B: Arctic Oscillation or North Atlantic Oscillation?, J.Clim., 14, 3495-3507, https://doi.org/10.1175/1520-0442(2001)014<3495:AOONAO>2.0.CO;2, 2001.
5. Andrade, C., and Belo-Pereira, M.: Assessment of droughts in the Iberian Peninsula using the WASP-Index. Atmos. Sci. Lett., 16, 208-218. https://doi.org/10.1002/asl2.542, 2015.
6. Barbeta, A., and Peñuelas, J.: Sequence of plant responses to droughts of different timescales: lessons from holm oak (Quercus ilex) forests, Plant. Ecol. Divers., 1-18, https://doi.org/10.1080/17550874.2016.1212288, 2016.
7. Barnston, A.G., and Livezey, R.E.: Classification, Seasonality and Persistence of Low-Frequency Atmospheric Circulation Patterns, Mon. Weather Rev., 115, 1083-1126, https://doi.org/10.1175/1520-0493(1987)115<1083:CSAPOL>2.0.CO;2, 1987.
8. Bueh, C., and Nakamura, H.: Scandinavian pattern and its climatic impact, Q. J. R. Meteorol. Soc., 133, 2117-2131, https://doi.org/10.1002/qj.173, 2017.
9. Casanueva, A., Rodríguez-Puebla, C., Frías, M.D., and González-Reviriego, N.: Variability of extreme precipitation over Europe and its relationships with teleconnection patterns. Hydrol. Earth Syst. Sci., 18, 709–725, https://doi.org/10.5194/hess-18-709-2014, 2014.
10. CHMLS(Confederación Hidrográfica delMiño-Sil). Plan especial de actuación en situaciones de alerta y eventual sequía, 2017. Documento Ambiental Estratégico (https://www.chminosil.es).
11. Cornes, R., van der Schrier, G. van den Besselaar, E.J.M., and Jones. P.D.: An Ensemble Version of the E-OBS Temperature and Precipitation Datasets, J. Geophys. Res. Atmos., 123, 1-52, https://doi.org/10.1029/2017JD028200, 2018.
12. Cortesi, N., Gonzalez-Hidalgo, J.C., Trigo, R.M., and Ramos, A.M.: Weather Types and spatial variability of precipitation in the Iberian Peninsula, Int. J. Climatol., 34, 2661-2677, https://doi.org/10.1002/joc.3866, 2014.
13. Dai, P. and Tan, B.: The Nature of the Arctic Oscillation and Diversity of the Extreme Surface Weather Anomalies It Generates, J. Climate, 30, 5563–5584, https://doi.org/10.1175/JCLI-D-16-0467.1, 2017.
14. deCastro, M., Lorenzo, N.G., Taboada, J.J., Sarmiento, M.E., Alvarez, I., and Gómez-Gesteira, M.: Influence of teleconnection patterns on precipitation variability and on river flow regimes in the Miño River basin (NW Iberian Peninsula), Clim. Res., 32, 63-73, https://doi.org/doi:10.3354/cr032063, 2006.
15. Dee, D.P., Uppala, S.M., Simmons, A.J., Berrisford, P., Poli, P., Kobayashi, S., Andrae, U., Balmaseda, M.A., Balsamo, G., Bauer, P., et al.: The ERA-Interim reanalysis: Configuration and performance of the data assimilation system. Q. J. R. Meteorol. Soc. 137, 553–597, https://doi.org/10.1002/qj.828, 2001.
16. Drumond, A., Nieto, R., Gimeno, L., Vicente-Serrano, S.M., and Lopez-Moreno, J.I.: Characterization of the atmospheric component of the winter hydrological cycle in the Galicia/North Portugal Euro-region: a Lagrangian approach, Clim. Res., 48, 193-201, https://doi.org/10.3354/cr00987, 2001.

https://doi.org/10.5194/nhess-2019-314
Preprint. Discussion started: 25 September 2019

17. Enfield, D.B., Mestas-Nunez, A.M., and Trimble, P.J.: The Atlantic Multidecadal Oscillation and its relationship to rainfall and river flows in the continental U.S., Geophys. Res. Lett., 28, 2077-2080, http://dx.doi.org/10.1029/2000GL012745, 2001.
18. García-Herrera, R., Hernández, E. Barriopedro, D. Paredes, D. Trigo, R.M., Trigo, I.F.,and Mendes, M.A.: The Outstanding 2004/05 Drought in the Iberian Peninsula: Associated Atmospheric Circulation, J. Hydrometeor., 8, 483–498, https://doi.org/10.1175/JHM578.1, 2007.
19. Gerber, N., and Mirzabaev, A.: Benefits of Action and Costs of Inaction: Drought Mitigation and Preparedness-A Literature Review, Technical report, World Meteorological Organization (WMO) and Global Water Partnership (GWP), doi:10.1201/9781315265551-8,2017.
20. Grinsted, A., Moore, J.C., and Jevrejeva, S.: Application of the cross wavelet transform and wavelet coherence to geophysical time series, Nonlin. Processes Geophys., 11, 561-566, https://doi.org/10.5194/npg-11-561-2004, 2004.
21. Gómez-Gesteira, M., Gimeno, L., deCastro M., Lorenzo, M.N., Alverez, I., Nieto, R., Taboada, J.J., Crespo, A.J.C., Ramos, A.M., Iglesias, I., Gómez-Gesteira, J.L., Sanro, F.E., Barriopedro, D., and Trigo, I.F.: The state of climate in NW Iberia. Clim. Res., 48, 109-144, https://doi.org/10.3354/cr00967, 2011.
22. González-Hidalgo, J.C., Vicente-Serrano, S.M., Peña-Angulo, D., Salinas, M., Tomas-Burguera, S., and Begueria, S.: High-resolution spatio-temporal analyses of drought episodes in the western Mediterranean basin (Spanish mainland, Iberian Peninsula). Acta Geophys., 66: 381-392, https://doi.org/10.1007/s11600-018-0138-x, 2018.
23. Gouveia, C., Trigo, R. M., and DaCamara, C. C.: Drought and vegetation stress monitoring in Portugal using satellite data, Nat. Hazards Earth Syst. Sci., 9, 185-195, https://doi.org/10.5194/nhess-9-185-2009, 2009.
24. Guerreiro, S.B., Dawson, R.J., Kilsby, C., Lewis, E., and Ford, A.: Future heat-waves,droughts and floods in 571 European cities, Environ. Res. Lett., 13, 1-11, https://doi.org/10.1088/1748-9326/aaaad3, 2018.
25. Hargreaves, G. H., and Samani, Z.: Reference crop evapotranspiration from temperature, Appl. Eng. Agric., 1, 96–99, https://doi.org/10.13031/2013.26773, 1985.
26. Hurrell, J.W.: Decadal trends in the North Atlantic Oscillation and relationships to regional temperature and precipitation, Science, 269, 676-679 , https://doi.org/10.1126/science.269.5224.676, 1995.
27. IPCC, 2018: Summary for Policymakers. In: Global Warming of 1.5°C. An IPCC Special Report on the impacts of global warming of 1.5°C above pre-industrial levels and related global greenhouse gas emission pathways, in the context of strengthening the global response to the threat of climate change, sustainable development, and efforts to eradicate poverty [Masson-Delmotte, V., P. Zhai, H.-O. Pörtner, D. Roberts, J. Skea, P.R. Shukla, A. Pirani, W. Moufouma-Okia, C. Péan, R. Pidcock, S. Connors, J.B.R. Matthews, Y. Chen, X. Zhou, M.I. Gomis, E. Lonnoy, T. Maycock, M. Tignor, and T. Waterfield (eds.)]. World Meteorological Organization, Geneva, Switzerland, 32 pp.
28. Knapp, A.K., Carroll, C.J.W., Denton, E.M., La Pierre, K.J., Collins, S.L., and Smith, M.D.: Differential sensitivity to regional-scale drought in six central US grasslands, Oecologia, 177, 949-957, https://doi.org/10.1007/s00442-015-3233-6, 2015.

https://doi.org/10.5194/nhess-2019-314
Preprint. Discussion started: 25 September 2019

29. Knudsen, M. F., Seidenkrantz, M.S., Jacobsen, B. H., and Kuijpers, A.: Tracking the Atlantic Multidecadal Oscillation through the last 8000 years, Nat. Commun., 2, 1-8, https://doi.org/10.1038/ncomms1186, 2011.
30. Lana, X., Martínez, M. D., Burgueño, A., Serra, C., Martín-Vide, J., and Gómez, L.: Distributions of long dry spells in the iberian peninsula, years 1951–1990, Int. J. Climatol., 26, 1999-2021, https://doi.org/10.1002/joc.1354, 2006.
31. Lehner, B., Verdin, K., and Jarvis, A.: New global hydrography de-rived from spaceborne elevation data, Eos, Transactions,89, 93–94, https://doi.org/10.1029/2008EO100001,2011.
32. Lorenzo-Lacruz, J., Morán-Tejeda, E., Vicente-Serrano, S. M., and López-Moreno, J. I.: Streamflow droughts in the Iberian Peninsula between 1945 and 2005: spatial and temporal patterns, Hydrol. Earth Syst. Sci., 17, 119-134, https://doi.org/10.5194/hess-17-119-2013, 2013.
33. López-Moreno, J. I., Vicente-Serrano, S.M., Zabalza, J., Begueria, S., Lorenzo-Lacruz, J., Azorin-Molina, C., and Morán-Tejeda, E.: Hydrological response to climate variability at different time scales: a study in the Ebro basin, J. Hydrol., 477, 175–188, https://doi.org/10.1016/j.jhydrol.2012.11.028, 2013.
34. Martens, B., Miralles, D.G., Lievens, H., van der Schalie, R., de Jeu, R.A.M., Fernández-Prieto, D., Beck, H.E., Dorigo, W.A., and Verhoest, N.E.C.: GLEAM v3: satellite-based land evaporation and root-zone soil moisture, Geosci. Model Dev., 10, 1903–1925, https://doi.org/10.5194/gmd-10-1903-2017, 2017.
35. McKee, T. B. N., Doesken, J., and Kleist, J.: The relationship of drought frequency and duration to time scales, Eight Conf. On Applied Climatology, Anaheim, California, United States, 179-184, 1993.
36. McMichael, A.J, and Lindgren, E.: Climate change: present and future risks to health, and necessary responses, J. Intern. Med., 270, 401-413, https://doi.org/10.1111/j.1365-2796.2011.02415.x, 2011.
37. Miralles, D.G., Holmes, T.R.H., de Jeu, R.A.M., Gash, J.H., Meesters, A.G.C.A., Dolman, A.J.: Global land-surface evaporation estimated from satellite-based observations, Hydrol. Earth Syst. Sci., 15, 453–469, doi: 10.5194/hess-15-453-2011, 2011.
38. Muñoz-Díaz, D., and Rodrigo, F. S.: Influence of the El Niño-Southern Oscillation on the probability of dry and wet seasons in Spain, Clim. Res., 30, 1–12, https://doi.org/10.3354/cr030001, 2004.
39. Ojeda, M. G-V., Jiménez,E.R., Gámiz-Fortis, S.R., Castro-Díez, Y., and Esteban Parra, M.J.: Understanding the Drought Phenomenon in the Iberian Peninsula, In book: Drought (Aridity) , https://doi.org/10.5772/intechopen.85472, 2019.
40. Parracho, A.C., Gonçalves, P.M., and Rocha, A.: Regionalisation of precipitation for the Iberian Peninsula and climate change, Phys. Chem. Earth, 54, 146-154, https://doi.org/10.1016/j.pce.2015.07.004, 2016.
41. Páscoa, P., Gouveia, C. M., Russo, A., and Trigo, R. M.: Drought Trends in the Iberian Peninsula over the Last 112 Years, Adv. Meteorol., 1-13, https://doi.org/10.1155/2017/4653126, 2017.
42. Peña-Gallardo, M., Vicente-Serrano, S.M., Camarero, J.J., Gazol, A., Sánchez-Salguero, R., Domínguez-Castro, F., El Kenawy, A., Beguería-Portugés, S., Gutiérrez, E., De Luis, M., Sangüesa-Barreda, G., Novak, K., Rozas, V., Tíscar, P.A., Linares, J.C., Martínez del Castillo, E., Ribas Matamoros, M., García-González, I., Silla, F., Camisón,

Á., Génova, M., Olano, J.M., Longares, L.A., Hevia, A., and Galván, J.D.: Drought Sensitiveness on Forest Growth in Peninsular Spain and the Balearic Islands, Forests, 9, 1-20, https://doi.org/10.3390/f9090524, 2018.

43. Peña-Gallardo, M., Vicente-Serrano, S. M., Domínguez-Castro, F., and Beguería, S.: The impact of drought on the productivity of two rainfed crops in Spain, Nat. Hazards Earth Syst. Sci., 19, 1215-1234, https://doi.org/10.5194/nhess-19-1215-2019, 2019.
44. Ramos, A.M., Cortesi, N., and Trigo, R.M.: Circulation weather types and spatial variability of daily precipitation in the Iberian Peninsula. Front. Earth Sci., 2, 1-17, https://doi.org/10.3389/feart.2014.00025, 2014.
45. Rivière, G., and Drouard, M.: Dynamics of the Northern Annular Mode at Weekly Time Scales, J. Atmos. Sci., 72, 4569–4590, https://doi.org/10.1175/JAS-D-15-0069.1, 2015.
46. Rodriguez-Puebla, C., Encinas, A.H., Nieto, S., and Garmendia, J.: Spatial and temporal patterns of annual precipitation variability over the Iberian Peninsula. Int. J. Climatol., 18, 299-316, https://doi.org/10.1002/(SICI)1097-0088(19980315)18:3<299::AID-JOC247>3.0.CO;2-L, 1998.
47. Russo, C., Gouveia, M., Trigo, R. M., Liberato, M. L., and DaCamara, C. C.: The influence of circulation weather patternsat different spatial scales on drought variability in the IberianPeninsula, Front. Environ. Sci., 3, 1-15, https://doi.org/10.3389/fenvs.2015.00001, 2015.
48. Salvador, C., Nieto, R., Linares, C., Díaz, J., and Gimeno, L.: Effects on daily mortality of droughts in Galicia (NW Spain) from 1983 to 2013, Sci. Total Environ., 662, 121-133, https://doi.org/10.1016/j.scitotenv.2019.01.217, 2019.
49. Schulte, E.M.m Grilo, C.M., and Gearhardt, A.N.: Shared and unique mechanisms underlying binge eating disorder and addictive disorders, Clin. Psychol. Rev., 44, 125-139, https://doi.org/10.1016/j.cpr.2016.02.001, 2016.
50. Serrano, A., García, J.A., Mateus, V.L., Cancillo, M.L., and Garrido, J.: Monthly modes of variation of precipitation over the Iberian Peninsula, J. Clim., 12, 2894-2919, https://doi.org/10.1175/1520-0442(1999)012<2894:MMOVOP>2.0.CO;2, 1999.
51. Smith, C.A., and Sardeshmukh, P.: The Effect of ENSO on the Intraseasonal Variance of Surface Temperature in Winter, Int. J. Climatol., 20, 1543 1557, https://doi.org/10.1002/1097-0088(20001115)20:13<1543::AID-JOC579>3.0.CO;2-A, 2000.
52. Sousa, P. M., Barriopedro, D., Trigo, R.M., Ramos, A.M., Nieto, R., Gimeno, L., Turkman, K. F., and Liberato, M.L.R.: Impact of Euro-Atlantic blocking patterns in Iberia precipitation using a novel high resolution dataset, Clim. Dyn., 46, 2573–2591, https://doi.org/10.1007/s00382-015-2718-7, 2016.
53. Spinoni, J., Naumann, G., Vogt, J., and Barbosa, P.: Meteorological droughts in Europe, Events and impacts, past trends and future projections, Publications Office of the European Union, Luxembourg, EUR 27748 EN, 129 pp., https://doi.org/10.2788/450449, 2016.
54. Stanke, C., Kerac, M., Prudhomme, C., Medlock, J., and Murray, V.: Health effects of drought: a systematic review of the evidence. PLoS Curr., 5, 1-22, https://doi.org/10.1371/currents.dis.7a2cee9e980f91ad7697b570bcc4b004, 2013.

https://doi.org/10.5194/nhess-2019-314
Preprint. Discussion started: 25 September 2019

55. Svoboda, M., Fuchs, B.: Handbook of Drought Indicators and Indices; World Meteorological Organization (WMO): Geneva, Switzerland; Global Water Partnership (GWP): Geneva, Switzerland, pp. 1–45 2016.
56. Thompson, D. W. J., and Wallace, J. M.: The Arctic Oscillation signature in the wintertime geopotential height and temperature fields, Geophys. Res. Lett., 25, 1297-1300, https://doi.org/10.1029/98GL00950, 1998.
57. Torrence, C. G., and Compo, P.: A practical guide to wavelet analysis. Bulletin of the American Meteorological Society, 79, 1, pp. 61–78, 1998.
58. Torrence, C. and Webster, P.J.: Interdecadal Changes in the ENSO–Monsoon System, J. Clim., 12, 2679–2690, https://doi.org/10.1175/1520-0442(1999)012<2679:ICITEM>2.0.CO;2, 1999.
59. Trenberth, K.E., Dai, A., Schrier, G., Jones, P.D., Barichivich, J., Briffa, K.R. and Sheffield, J. Global warming and changes in drought, Nat. Clim. Change, 4, 17– 22, https://doi.org/10.1038/nclimate2067, 2014.
60. Trigo, R.M., and DaCamara, CC.: Circulation weather types and their influence on the precipitation regime in Portugal, Int. J. Climatol., 20, 1559–1581, https://doi.org/10.1002/1097-0088(20001115)20:13<1559::AID-JOC555>3.0.CO;2-5, 2000.
61. Trigo, R.M., Osborn, T.J., and Corte-Real, J.: The North Atlantic Oscillation influence on Europe: Climate impacts and associated physical mechanisms, Clim., Res., 20, 9-17, https://doi.org/10.3354/cr020009, 2002.
62. Trigo, R. M., Pozo-Vázquez, D., Osborn, T. J., Castro-Díez, Y., Gámiz-Fortis, S., and Esteban-Parra, M. J.: North Atlantic oscillation influence on precipitation, river flow and water resources in the Iberian Peninsula. Int. J. Climatol., 24, 925-944, https://doi.org/doi:10.1002/joc.1048, 2004.
63. Van Lanen, H.A.J.: Drought propagation through the hydrological cycle. Climate Variability and Change—Hydrological Impacts, in: Proceedings of the Fifth FRIEND World Conference , Havana, Cuba, November, 2006, 308, 2006.
64. Vargas, J., and Paneque, P.: Challenges for the Integration of Water Resource and Drought-Risk Management in Spain, Sustainability, 11, 1-16, https://doi.org/10.3390/su11020308, 2019.
65. Vicente-Serrano, S.M., Beguería, S., and López-Moreno, J.I.: A Multiscalar Drought Index Sensitive to Global Warming: The Standardized Precipitation Evapotranspiration Index, J. Clim., 23, 1696–1718, https://doi.org/10.1175/2009JCLI2909.1, 2010.
66. Vicente-Serrano, S. M.: El Niño and La Niña influence on droughts at different timescales in the Iberian Peninsula, Water Resour. Res., 41, 1-18, https://doi.org/10.1029/2004WR003908, 2005.
67. Vicente-Serrano, S. M., López-Moreno, J. I., Bergueria, S., Lorenzo-Lacruz, J., Sanchez-Lorenzo, A., García-Ruiz, J.M., Azorin-Molina, Morán-Tejeda, E., Revuelto, J., and Trigo, R.: Evidence of increasing drought severity caused by temperature rise in southern Europe, Environ. Res. Lett., 9, 1-14, https://doi.org/10.1088/1748-9326/9/4/044001, 2014.

https://doi.org/10.5194/nhess-2019-314
Preprint. Discussion started: 25 September 2019

68. Vicente-Serrano, S.M., López-Moreno, J.I., Drumond, A., and Gimeno, L., Nieto, R., Morán-Tejeda, E., Lorenzo-Lacruz, J., Begueria, S., and Zabalza, J.: Effects of warming processes on droughts and water resources in the NW Iberian -Peninsula (1930−2006). Clim. Res., 48, 203-212, https://doi.org/10.3354/cr01002, 2011.

69. Vicente-Serrano, S.M., López-Moreno, J.I., Santiago, B., Lorenzo-Lacruz, J., Azorin-Molina, C., and Morán-Tejeda, E.: Accurate computation of a streamflow drought index, J. Hydrol. Eng., 17, 318–332, https://doi.org/10.1061/%28ASCE%29HE.1943-5584.0000433, 2012.

70. Vidal-Macua J.J., Ninyerola M., Zabala A., Domingo-Mari-mon C., and Pons, X.: Factors affecting forest dynamics in the Iberian Peninsula from 1987 to 2012. The role of topography and drought, For. Ecol. Manag., 406, 290–306, https://doi.org/10.1016/j.foreco.2017.10.011, 2017.

71. Visbeck, M.H., Hurrell, J.W., Polvani, L., and Cullen, H.M.: The North Atlantic Oscillation: Past, present, and future, Proc. Natl. Acad. Sci. U.S.A., 98, 12876–12877, https://doi.org/10.1073/pnas.231391598, 2001.

72. Wang, W., Ertsen, M.W., Svoboda, M.D., and Hafeez, M.: Propagation of Drought: From Meteorological Drought to Agricultural and Hydrological Drought, Adv. Meteorol.,2016, 1-5, http://dx.doi.org/10.1155/2016/6547209, 2016.

73. Wanner, H., Brönnimann, S., Casty, C., Gyalistras, D., Luterbacher, J., Schmutz, C., Stephenson, D.B., and Xoplaki, E.: North Atlantic Oscillation – Concepts and Studies, Surv. Geophys., 22, 321–381, https://doi.org/10.1023/A:1014217317898, 2001.

74. Wilhite, D. A.: Drought as a Natural Hazard: Concepts and Definitions. Drought: A Global Assessment, edited by Wilhite, D.A., Natural Hazards and Disasters Series, Routledge, London, U.K., 3-18, 2000.

75. World Meteorological Organization. Standardized Precipitation Index User Guide. 2012. Available online: http://www.wamis.org/agm/pubs/SPI/WMO_1090_EN.pdf (accessed on 08 September 2019).

76. World Meteorological Organization (WMO) and Global Water Partnership (GWP), 2016: Handbook of Drought Indicators and Indices (M. Svoboda and B.A. Fuchs). Integrated Drought Management Programme (IDMP), Integrated Drought Management Tools and Guidelines Series 2. Geneva.